energies

MDPI

Article

Experimental Investigation of Neat Biodiesels' Saturation Level on Combustion and Emission Characteristics in a CI Engine

Vikas Sharma [1], Abul K. Hossain [1,*] and Ganesh Duraisamy [2]

[1] Aston Institute for Urban Technologies and the Environment (ASTUTE), Department of Mechanical, Biomedical & Design Engineering, College of Engineering & Physical Sciences, Aston University, Birmingham B4 7ET, UK; v.sharma10@aston.ac.uk

[2] Internal Combustion Engine Division, Department of Mechanical Engineering, College of Engineering, Anna University, Chennai 600025, Tamil Nadu, India; ganvas12@annauniv.edu

* Correspondence: a.k.hossain@aston.ac.uk

Abstract: The fuel qualities of several biodiesels containing highly saturated, mono, and poly unsaturated fatty acids, as well as their combustion and exhaust emission characteristics, were studied. Six biodiesel samples were divided into two groups based on their fatty acid composition, including group 1 (coconut, castor, and jatropha) and group II (palm, karanja, and waste cooking oil biodiesel). All fuels (in both groups) were tested in a single-cylinder off-road diesel engine. Castor and karanja biodiesel, both rich in mono-unsaturation level, have a high viscosity of about 14.5 and 5.04 mm^2/s, respectively. The coconut and palm biodiesels are rich in saturation level with cetane numbers of 62 and 60, respectively. In both groups, highly saturated and poly-unsaturated methyl esters presented better combustion efficiency and less formation of polluted emissions than mono-unsaturation. At full load, coconut and palm biodiesel displayed 38% and 10% advanced start of combustion, respectively, which reduced ignition delay by approximately 10% and 3%, respectively. Mono-unsaturated methyl esters exhibited a higher cylinder pressure and heat release rate, which results in higher NOx gas emissions. The group II biodiesels showed about 10–15% lower exhaust emissions owing to an optimum level of fatty acid composition. Our study concluded that highly saturated and poly-unsaturated fatty acid performed better than mono-unsaturated biodiesels for off-road engine application.

Keywords: biofuels; biodiesel saturation; carbon bonding; combustion; emission; engine; performance; renewable fuels; waste

Citation: Sharma, V.; Hossain, A.K.; Duraisamy, G. Experimental Investigation of Neat Biodiesels' Saturation Level on Combustion and Emission Characteristics in a CI Engine. *Energies* **2021**, *14*, 5203. https://doi.org/10.3390/en14165203

Academic Editors: Luis Hernández-Callejo and Attilio Converti

Received: 23 June 2021
Accepted: 17 August 2021
Published: 23 August 2021

1. Introduction

Recently, there has been a lot of focus on environmental pollution and rapid reduction in fossil fuel resources [1]. Worldwide, this has become an important challenge, and several techniques for reducing the negative consequences of fossil fuel emissions have been proposed [2]. Researchers are continuously working to find solutions to replace conventional fossil-based diesel fuel [3]. Fossil fuels generate a considerable amount of pollutant gases, which have caused global warming, as well as negative impacts on human health and other living beings [4]. The combustion of fossil fuels produces harmful pollution such as nitrogen oxides (NOx), hydrocarbons (HC), sulphur dioxide (SO_2), carbon monoxide (CO), particulate matter (PM), and carbon dioxide (CO_2) [5]. Human toxicity has been established for several hazardous contaminants. In 2007–2020, the combustion of fossil fuels resulted in the release of 4.1 million metric tonnes of CO_2 globally [6]. Countries in the EU (European Union) alone consume nearly 25.7% of energy in residential sectors responsible for huge CO_2 emission [7]. Renewable fuels, such as biodiesel, have been proposed to replace petroleum fossil fuels to reduce global CO_2 emissions. Biodiesel is non-toxic and environmentally beneficial [8]. Furthermore, when compared with fossil fuels, biodiesel fuel can cut CO_2 emissions by about 78.45% [8]. Biodiesel is an alternative

sustainable source, which can be produced from plant seed oils, animal fats, and other long-chain fatty acid containing substances such as waste cooking oil [9]. In addition, biodiesels are also used as an additive to improve the lubricity property of fossil diesel [9]. Saturated (SFA), monounsaturated (MUFA), and polyunsaturated (PUFA) fatty acids are the three types of fatty acids (FAs) found in biodiesel [10]. The SFAs are those that have single (C–C) bonds, while USFAs contain double (C=C) bonds [10]. The unsaturated fatty acids (USFAs) are classified into two types: MUFAs with only one (C=C) double bond and PUFAs with more than two (C=C) double bonds [11]. As the number of double bonds increases, the melting temperature decreases, hence USFAs have a lower melting point than SFAs [10]. Chemical reactivity increases as the amount of double bonds increases; thus, USFAs are more chemically reactive than SFAs [10]. Puhan et al. (2010) studied the impact of three biodiesels with distinct molecular architectures on combustion and emission parameters in a stationary diesel engine. Linseed, jatropha, and coconut oils were used to make the biodiesels. They found that, as the degree of unsaturation of biodiesels increased, the ignition delay (ID) and exhaust gas temperatures increased [12]. They found that, owing to significant NOx emissions and low thermal efficiency, linseed biodiesel is not suitable for use in diesel engines [12]. Sochonborn et al. (2009) examined the effect of fatty acid methyl-ester combustion behavior in a single-cylinder research engine [13]. They reported that the carbon chain structure of the methyl ester had a significant impact on NOx emissions [13]. Kruczynski (2013) investigated Camelina biodiesel–diesel blends in a direct injection diesel engine [14]. They revealed that, as the composition of biodiesel increased, the ignition delay and heat release decreased [14]. They observed that, when the biodiesel percentage in the blend increased, NOx, HC, CO, CO_2, and smoke emissions increased [14]. Fuel properties directly influence the fuel combustion and emission characteristics. Zhang et al. (2009) investigated the premixed combustion behavior of four carbon methyl esters in a research engine [15]. They examined the impact of low-temperature fuel oxidation on exhaust gases at different compression ratios [15]. The authors reported that, owing to the existence of (C=C) double bonds in the fatty acid carbon chain, the tested fuels exhibited different ignition behaviors [15].

Selvam and Nagrajan (2013) evaluated the combustion characteristics of higher SFA biodiesel fuel [16]. Pongamia, rice bran, sunflower, and palm oil were used to make the biodiesels. They observed that biodiesel with a high SFA has a higher cetane number, which improves the fuel's combustion efficiency [16]. Furthermore, they determined that, the higher the SFA level in biodiesel, the lower the NOx formation. Most of the studies found in the literature were focused on biodiesel–diesel blends, biodiesel–alcohol blends, and biodiesel–diesel with additives, whereas, very few studies were found investigating the combustion characteristics of 100% biodiesels (neat biodiesel) based on their fatty acids' compositions. In addition, there is a clear gap in the literature on how the three levels of biodiesel saturation (highly saturated, mono-unsaturated, and poly-unsaturated) affect the combustion and emission characteristics. Furthermore, studies reported in the literature were performed in various types of diesel engines (with different operating parameters such as compression ratios, injection timings, and so on). When testing the neat biodiesels with different saturation levels in the same engine (i.e., same operating parameters of the engine), it is essential to investigate the combustion and emission characteristics of neat biodiesel fuels. Hence, the aim of this study is to examine the combustion and emission behavior of the highly saturated, mono-unsaturated, and poly-unsaturated methyl esters in the same diesel engine. Furthermore, a parameter, known as the degree of unsaturation (DU) (product of mono and poly unsaturation), is used. The combustion characteristics of biodiesel will also be examined in this study, which are dependent on the percentage of DU. A single-cylinder stationary variable compression ratio diesel engine was use for the biodiesel test with varied saturation levels. The objectives of this investigation are as follows: (i) to produce biodiesels with various levels of saturation; (ii) the measurement and comparison of the biodiesels' fuel properties based on their saturation levels; (iii) to further understand the behavior of FAME compositions, investigating the combustion and

emission characteristics of neat biodiesels under the same engine operating conditions; and (iv) to study the effect of degree of unsaturation on combustion and emission characteristics. Six biodiesel fuels were used based on their fatty acids' profile: coconut, palm, castor, karanja, jatropha, and waste cooking oil biodiesel. These six biodiesel samples are divided into two groups: (i) group I, fuels containing very high saturated, mono-unsaturated, and poly-unsaturated methyl esters; (ii) group II, fuels containing low saturated, mono-unsaturated, and poly-unsaturated methyl esters. Finally, the combustion and emission qualities of biodiesels will be compared in order to determine the correlations between the various saturation levels.

2. Materials and Methods

Six oil samples were selected for biodiesel production based on the availability in the market (in India): four non-edible, one edible, and waste cooking oil. The required chemicals such as sulfuric acid and potassium hydroxide (KOH) were procured from the Sigma-Aldrich (Bengaluru, India). The methanol was procured from Alpha Chemika (Mumbai, India). Biodiesel and diesel fuel samples were characterized in the biofuel laboratory of the institute (at Anna University). For combustion and emission characterization, a variable compression ratio (VCR) engine was utilized. For this study, only neat biodiesels were tested in the engine. Based on the FAME compositions, these biodiesel fuels were divided into two groups (group 1 and group 2). Group 1 refers to highly saturated and group 2 refers to low saturated esters. Furthermore, in each group, biodiesels were categorized as SFA, MUFA, and PUFA esters. Group 1 contains highly saturated esters (high SFA (coconut), high MUFA (castor), and high PUFA (jatropha)), whereas group 2 contains low saturated esters (low SFA, (palm), low MUFA (karanja), and low PUFA (WCO)).

2.1. Biodiesel Production

A laboratory setup with a 5 L capacity was used to make biodiesel (Figure 1). A two-stage chemical process was selected owing to the presence of a high level of free fatty acids (FFA%) in non-edible oils. The acid catalysis (esterification) procedure was employed to lower the FFA content in the first stage. In the esterification process, a methanol-to-oil 6:1 molar ratio was added to the warmed oil (at 60 °C), along with 2% sulphuric acid (H_2SO_4) (v/v). The mixture was agitated for 3 h at 600 rpm.

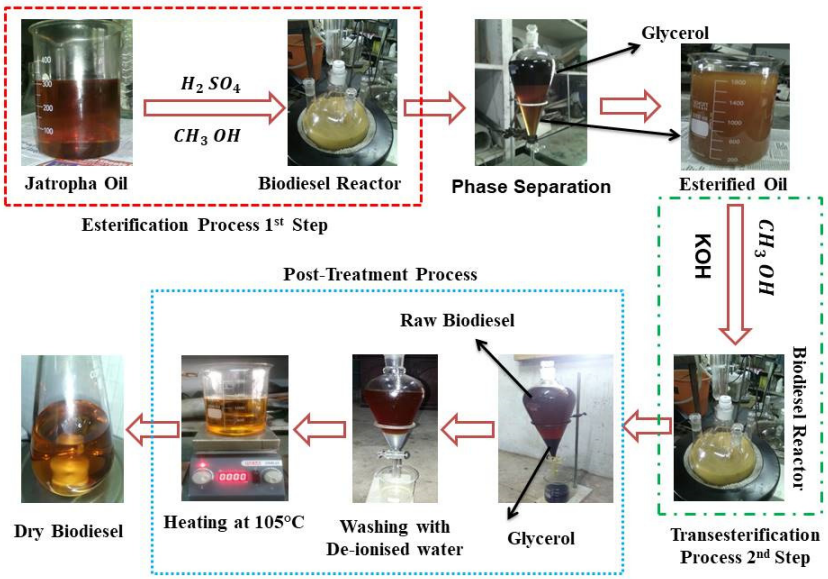

Figure 1. Two-stage biodiesel production process (jatropha biodiesel).

After the reaction was completed, the mixture was transferred to a separating flask and allowed to settle overnight. The bottom layer contained esterified oil, whereas the

upper layer contained glycerol. The esterified oil was separated and kept warm (100 °C) until the moisture and excess methanol were removed. After that, the second stage, known as the base catalysis process (i.e., transesterification), was employed. A methanol-to-oil 4:1 molar ratio with 1% KOH (*w*/*w*), was added to the preheated oil at 60 °C and agitated for 1 h at 600 rpm (Figure 1). The mixture was then transferred to a separating flask where the glycerol and methyl ester were separated. To eliminate any leftover methanol, soap, catalyst, or glycerol, the raw biodiesel sample was rinsed with hot distilled water (at 70 °C). Finally, the methyl ester was heated to 105 °C for 1 h to eliminate any remaining moisture, yielding a pure dry methyl ester (Figure 1).

Characterisation of Biodiesel Fuel

The equipment and measurement standards used for fuel characterisation are shown in Table 1. Gas chromatography and mass spectrometry (GC-MS) was used at IIT Madras (India) to determine the percentage of fatty acids methyl ester (FAME) composition. The FAME profile was used to calculate SFA, MUFA, PUFA, and DU percentages using Equations (1)–(5). The degree of unsaturation (DU) refers to the average number of double bonds in a compound [17]. The cetane number was estimated using Equation (6) from the FAME profile [18]. A closed cup method was used to determine the flash point temperature of the fuel samples. The iodine value was determined using a titration method in the biofuel lab.

$$\text{SFA\%} = \sum \text{C} - \text{C}\ \textit{single bond in FAs} \quad (1)$$

$$\text{MUFA\%} = \sum \text{C} = \text{C}\ \textit{double bond in FAs} \quad (2)$$

$$\text{PUFA\%} = \sum \textit{More then one}\ (-\text{C} = \text{C}-)\ \textit{bouble bond in FAs} \quad (3)$$

$$\text{USFA\%} = \text{MUFA} + \text{PUFA} \quad (4)$$

$$\text{DU} = \text{MUFA}\ \% + (2 \times \text{PUFA}\ \%) \quad (5)$$

$$\text{CN} = 62.2 + (0.017 \times \text{C12}:0) + (0.074 \times \text{C14}:0) + (0.0115 \times \text{C16}:0) + (0.077 \times \text{C18}:0) - (0.101 \times \text{C18}:1) - (0.279 \times \text{C18}:2) - (0.366 \times \text{C18}:3) \quad (6)$$

Table 1. List of the equipment and standards used for fuel characterisation.

Fuel Properties	Name of the Instrument	Standards
Density	Hydrometer	BIS ISO1448
Kinematic viscosity	Redwood viscometer	BIS ISO1448
Calorific value	Bomb calorimeter	BIS ISO1448-6
Oxidation stability	Rancimat method	EN 14112 (AOCS Cd 12b-92)
Iodine value	Titration method	EN 14111
Flash point	Closed cup	EN 3679
Acid value	Titration method	BIS ISO 7537

2.2. Experimental Test Rig

A single cylinder variable compression ratio (VCR) diesel engine was used for testing (Table 2). Figure 2 depicts the test rig. To provide load to the engine, an eddy current dynamometer was connected to it. The engine was coupled with eddy current dynamometer, which was calibrated by applying the load to the dynamometer arm. Then, the load indicator was calibrated. The load was applied to the engine through an eddy current dynamometer. The engine test was carried out at 1500 rpm at a constant compression ratio of 17.5. Three engine loads were set for experiments such as 0% (no/idle load), 50% (medium, 12 Nm), and 100% (full load, 24 Nm). An orifice meter and a U-tube manometer were used to measure airflow. The fuel flow was measured using a real-time fuel consumption meter with an optical sensor. Thermocouples (K-type) were used to measure the temperatures of the engine exhaust gas, air, and water coolant. All signals were recorded by a lab-view-based application that displayed airflow, fuel flow, temperatures, and other

performance data in real time. A Kistler pressure transducer (Kistler 6013C, 0–100 bar) was used to measure in-cylinder pressure, whereas an Autonics crank angle encoder (1 °C A resolution) was used to detect the crank angle position. The concentration of various gases present in the engine exhaust was measured using a HORIBA (MEXA 584L) gas analyzer. Table 3 shows the HORIBA gas analyzer's technical specification. An AVL (AVL 437) smoke meter was used to determine the smoke opacity of the exhaust gas (Table 3).

Table 2. Technical specification of the engine.

Rated Power	5 HP @1500 rpm
Number of cylinder	1
Stroke (mm)	110
Compression ratio (variable)	17.5:1 (12:1 to 22:1)
Original displacement (cc)	661.4
Combustion chamber volume (cc)	Variable
Piston bowl diameter (mm)	49.5
Piston bowl height (mm)	23.5
Number of holes in injector	3
Start of injection (SOI)	23° bTDC

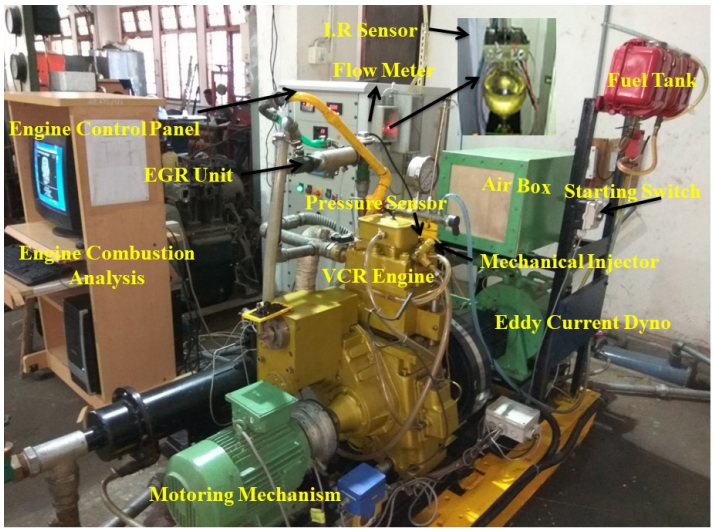

Figure 2. Photographic view of the diesel engine test rig.

Table 3. Technical specifications of various instruments.

Instrument	Measured Parameters	Range	Uncertainty
Horiba Gas Analyser (MAXA 584L)	CO	0–10% vol	±0.01%
	CO_2	0–20% vol	±0.17
	HC	0–20,000 ppm	±3.3 ppm
	NO	0–5000 ppm	±0.5 ppm
	O_2	0–25%	±0.5%
Smoke Meter (AVL 437)	Smoke opacity	0–100 opacity	±1%
Pressure Sensor Kistler-6613CQ09	Cylinder pressure	0–100 bar	±1%
Autonics Encoder (Rotary Type)	Crank angle	360° revolution	5VDC-12VDC ± 0.5%
K-type Thermocouple	Temperature	0 °C–400 °C	2.2 °C, or ±2%

3. Results and Discussions

3.1. Fuels Characteristics

Tables 4 and 5 illustrate the physical and chemical parameters of the neat biodiesel. Table 5 shows the GCMS analysis of the fatty acid profile of biodiesels; these values are used to calculate the SFA, MUFA, PUFA, and DU percentages as shown in Table 4. The saturation

levels of the biodiesel varied widely; in general, they are inversely related to the degree of unsaturation (Table 4). It was revealed that, when the degree of unsaturation decreases, the saturation levels rise (Table 4). In general, the cetane number increased with the decrease in DU levels [17]. The cetane number of the karanja, jatropha, and WCO biodiesels are close to each other because they have almost similar levels of DU (Table 4). However, the castor biodiesel shows a slightly lower cetane number; the reason for this is that the castor biodiesel contains about 88% of ricilonic acid (C18:1, OH), which led to having higher MUFA and lower SFA and PUFA levels (Tables 4 and 5). The presence of the OH group in the chemical structure decreased the ignition quality of castor biodiesel [17]. No trend was observed for HHV and density values. The flash point temperature and iodine values increased with the increase in DU levels (Table 4). The oxidation stability depends on the amount of PUFA; the higher the PUFA, the lower the oxidation stability (Table 4).

Table 4. Fuel properties of various biodiesels.

Biodiesel	Coconut	Palm	Karanja	WCOB	Jatropha	Castor	Biodiesel Standards	
							EN 14214:2012	ASTM D6751-12
Cetane number	62	60	55.4	56.2	55.8	42.1	min. 51	min. 47
Density (kg/m^3)	868.8	874.7	882.9	880.6	878.7	917.6	860–900	-
HHV (KJ/kg)	38,725	39,485	40,125	39,805	40,380	39,980	-	-
Viscosity (mm^2/s) at 40 °C	2.78	4.61	5.04	4.75	4.72	14.5	3.5–5.0	1.9–6.0
Flash point °C	123	169	159	161	172	179	min. 101	min. 93
Iodine value (g Iod/100 g)	7.8	52.7	85.5	85.1	99	85.2	max. 120	-
Oxidation stability (h)	11	11.4	4.1	5	5	12.9	8 h min.	3 h min.
Acid number (mgKOH/g)	0.16	0.27	0.44	0.41	0.34	0.39	max. 0.50	max. 0.50
SFA (%)	90.31	48.56	24.65	24.03	22.12	2.76	-	-
MUFA (%)	6.45	41.22	52.30	44.58	42.28	91.84	-	-
PUFA (%)	3.24	10.22	23.05	31.39	35.60	5.4	-	-
USFA (%)	9.69	51.44	75.35	75.97	77.88	97.24	-	-
DU (%)	12.93	61.66	98.4	107.36	113.48	102.64	-	-

Table 5. FAME composition of various biodiesels.

Biodiesel Fatty Acids		Coconut	Palm	Karanja	WCOB	Jatropha	Castor
C8:0	Caprylic	6.46	0.08	0	0	0	0
C10:0	Capric	5.62	0.06	0	0	0	0
C12:0	Luric	46.90	0.37	0	0.2	0	0
C14:0	Myristic	18.70	1.13	0	0.67	0.15	0
C16:0	Palmitic	9.69	42.39	10.89	15.69	14.40	1.38
C16:1	Palmitoleic	0.18	0.16	0	0.74	0.67	0
C17:0	Margaric	0	0.06	0	0.2	0.08	0
C18:0	Stearic	2.84	4.2	7.2	6.14	5.80	1.11
C18:1	Oleic	6.27	40.90	51.15	42.84	42.51	3.35
C18:2	Linoleic	3.24	9.95	21.01	29.36	35.37	4.84
C18:3	Linolenic	0	0.27	2.04	2.03	0.23	0.56
C20:0	Arachidic	0.1	0.22	1.12	0.39	0.08	0.26
C20:1	Gadoleic	0	0.16	1.15	0.75	0.1	0.42
C22:0	Bahenic	0	0	4.11	0.44	0.14	0
C22:1	Erucic	0	0	0	0.25	0	0
C24:0	Lignoceric	0	0.05	1.33	0.3	1.47	0
C18:1, OH	Ricinoleic	-	-	-	-	-	88.06

3.2. Combustion Characteristics

Start of combustion (SoC), end of combustion (EoC), ignition delay (ID), combustion duration (CD), in-cylinder pressure, rate of pressure rise, heat release rate, cumulative heat release, and mass fraction burned (MFB) were used to characterize the combustion behavior of biodiesel fuels.

3.2.1. Start and End of Combustion

The mass fraction of combusted fuel was used to compute the SoC and EoC, as illustrated in Figure 3. The SoC was assumed where 5% of the fuel has burned, and the EoC was assumed where 90% of the fuel has burned with respect to the crank angle degree [13]. Because of the presence of oxygen and higher CN, biodiesel fuel showed earlier SoC timing. As the engine load increased, the SOC advanced (Figure 3). Advanced SoC was observed for SFA (coconut and palm biodiesel) as compared with MUFA and PUFA methyl esters. The sequence of SoC was observed as follows: SFA > MUFA > PUFA (Figure 3). In group I, coconut biodiesel started burning earlier by 76% and 20%, 57% and 10%, and 38% and 3.84%, as compared with castor and jatropha biodiesel at 0%, 50%, and 100% loads, respectively (Figure 3). Coconut biodiesel has a higher SFA, CN, and viscosity than jatropha and castor biodiesel, resulting in this feature (Table 4) [12], whereas jatropha biodiesel started burning earlier by 70%, 52%, and 36% than the castor biodiesel at 0%, 50%, and 100% load, respectively. In group II, palm biodiesel started burning earlier by 27% and 37%, 11% and 17%, and 10% and 12% than karanja and WCOB biodiesel at 0%, 50%, and 100% load, respectively. It is owing to the higher SFA and CN (Table 4) [19]. Karanja biodiesel started burning slightly earlier by 14%, 6%, and 2% than WCOB at 0%, 50%, and 100% load, respectively, as shown in Figure 3.

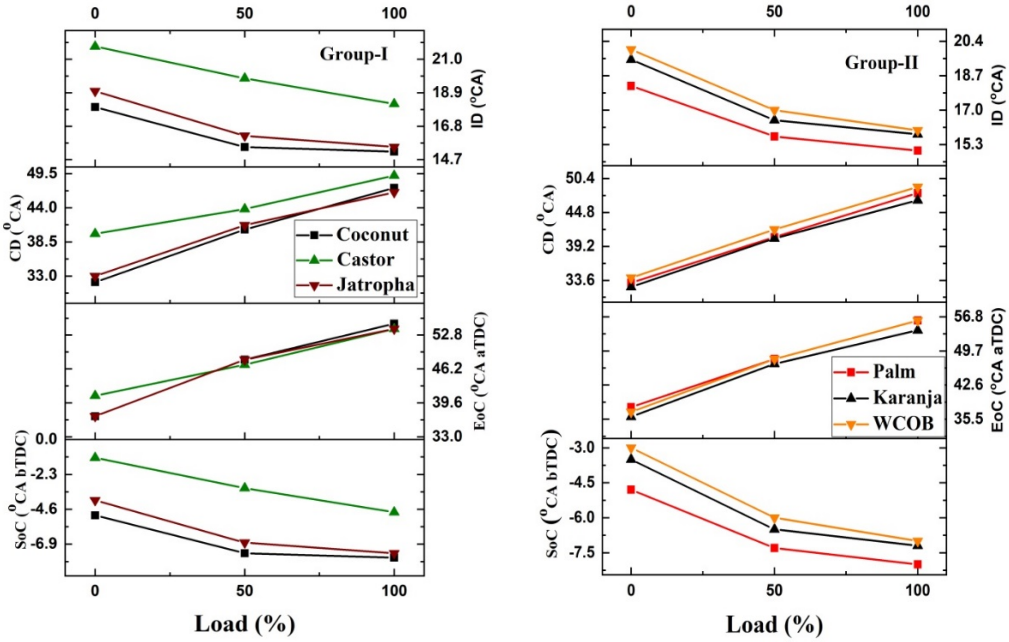

Figure 3. Combustion characteristics for group I and group II saturated fatty acid methyl esters.

The MUFA (castor biodiesel) showed retardation in SoC compared with PUFA (jatropha) (Figure 3). Castor oil consists of highly mono-unsaturated fatty acids with 88% ricinoleic acid (Table 5). The high ricinoleic acid caused higher viscosity and a lower cetane number [20]. The viscosity of castor biodiesel is very high (14 mm^2/s) as compared with other biodiesel samples. The high viscous fuel affects the fuel spray characteristics such as fuel droplet size, atomization, and evaporation [20]. Fuel with large droplet size took a slightly longer time to evaporate and form a flammable combination [20]. Therefore, in all load conditions, SoC of castor biodiesel was delayed compared with other biodiesel samples. In general, the EoC increased with load, as shown in Figure 3. At each load condition, there were nearly identical for all biodiesels. The EoC of castor biodiesel, on the other hand, was found to be greater at no load. Castor biodiesel, for example, has a higher viscosity and density (Tables 4 and 5), resulting in a higher EoC [21]. Under the no load condition, the in-cylinder temperature is low; hence, the combined effects of low in-cylinder temperature and higher viscosity gave higher EoC for castor biodiesel.

With increased engine load, the ignition delay was shortened (Figure 3). Except castor biodiesel, the ID period of SFA (coconut and palm) was shorter than that of MUFA and PUFA biodiesels (Figure 3). The ID period dropped as the engine load increased owing to an increase in-cylinder temperature. The duration of the physical delay was reduced when the cylinder temperature was raised; hence, the ID period was shortened [22]. Owing to its higher viscosity and lower CN, castor biodiesel had a longer ID period (21.8 °CA) than the other samples (Table 4). The CD is prolonged as the engine load increases because of increased the amount of fuel per cycle (Figure 3). In general, the CD for all biodiesel samples was almost similar at all the engine load conditions except castor biodiesel (Figure 3). Because of the high kinematic viscosity and less CN (Table 4), castor biodiesel gave highest CD of 49.2 °CA at full load. The CD of SFA was found to be slightly lower than MUFA and PUFA (Figure 3).

Figure 4 shows the mass fraction burnt (MFB) for various biodiesels. From group I, at 0% load, it was observed that highly SFA (coconut) gave higher MFB as compared with PUFA (jatropha) and MUFA (castor) biodiesels (Figure 4). Higher CN and lower viscosity of higher SFA biodiesel (coconut) results in advanced SOC and a shorter ID period. At 0% load, in-cylinder temperature was lower, which reduces the fuel oxidation rate (atomization and vaporization). In the case of castor biodiesel and at 0% load, ignition delay is longer than that of coconut and jatropha (Figure 3) owing to the higher viscosity; because of this, the MFB rate for castor biodiesel was lower than other biodiesels (Table 4) [23]. On the other hand, at 50% and 100% load, the MFB rate for higher MUFA (castor) fuel was faster than PUFA (jatropha) and SFA (coconut) fuels. It is because of longer ID, which allow more fuel to burn in the pre-mixed combustion phase, which results in a higher rate of Pmax and HRRmax (Figure 4). It was believed that a longer ID at high engine loads accelerated the MFB rate [23]. A similar trend was also observed in group II fuels (Figure 4). Palm biodiesel has a higher CN and lower viscosity than Karanja and WCOB. This aids in the early ignition of combustion and reduces the ignition delay [20]. It means less fuel is burned in the premix combustion phase and more fuel will burn in the diffusion combustion or late combustion phase. These results lower the rate of combustion efficiency as in-cylinder temperature reduced in expansion and exhaust stroke, which reduced the fuel oxidation rate [20]. It can be observed from Figure 3 that the SoC of Palm biodiesel is more advanced than other samples; in Figure 5, the Pmax and HRRmax for palm are lower at 50% and 100%, respectively. This results in a lower MFB rate of palm biodiesel at 50% and 100% load.

3.2.2. In-Cylinder Pressure

In group I, it was observed that, at 0% load, the coconut biodiesel (highly SFA) gave 17% and 2.8% higher in-cylinder pressure than castor and jatropha, respectively (Figures 5 and 6). The reason behind this was that coconut biodiesel had a higher CN (i.e., advanced SoC) and lower viscosity characteristics, which improved the combustion efficiency during low in-cylinder temperature [24] (Figure 3, Table 4). At 0% load, jatropha biodiesel (high PUFA) produced 2.8% lower in-cylinder pressure than coconut, but 15% higher than castor biodiesel (high MUFA). At 50% load, jatropha biodiesel (highly PUFA) gave 0.4% higher peak in-cylinder pressure as compared with coconut and castor biodiesels, whereas at 100% load, castor biodiesel (highly MUFA) gave 4.5% and 2.1% higher peak in-cylinder pressures than coconut and jatropha biodiesels (Figures 5 and 6). A higher MFB of castor biodiesel at 100% load (Figure 4) caused this. In group II and at 0% load, palm biodiesel (SFA) gave 1.28% and 1.15% higher in-cylinder pressures than karanja (MUFA) and WCOB (PUFA) biodiesels, respectively. At 50% load, WCOB (PUFA) gave 3.2% and 0.6% higher peak in-cylinder pressure than SFA and MUFA, respectively. When compared with SFA and MUFA, the Pmax of WCOB (PUFA) was increased by 1.3% and 0.4%, respectively, at 100% load (Figure 6).

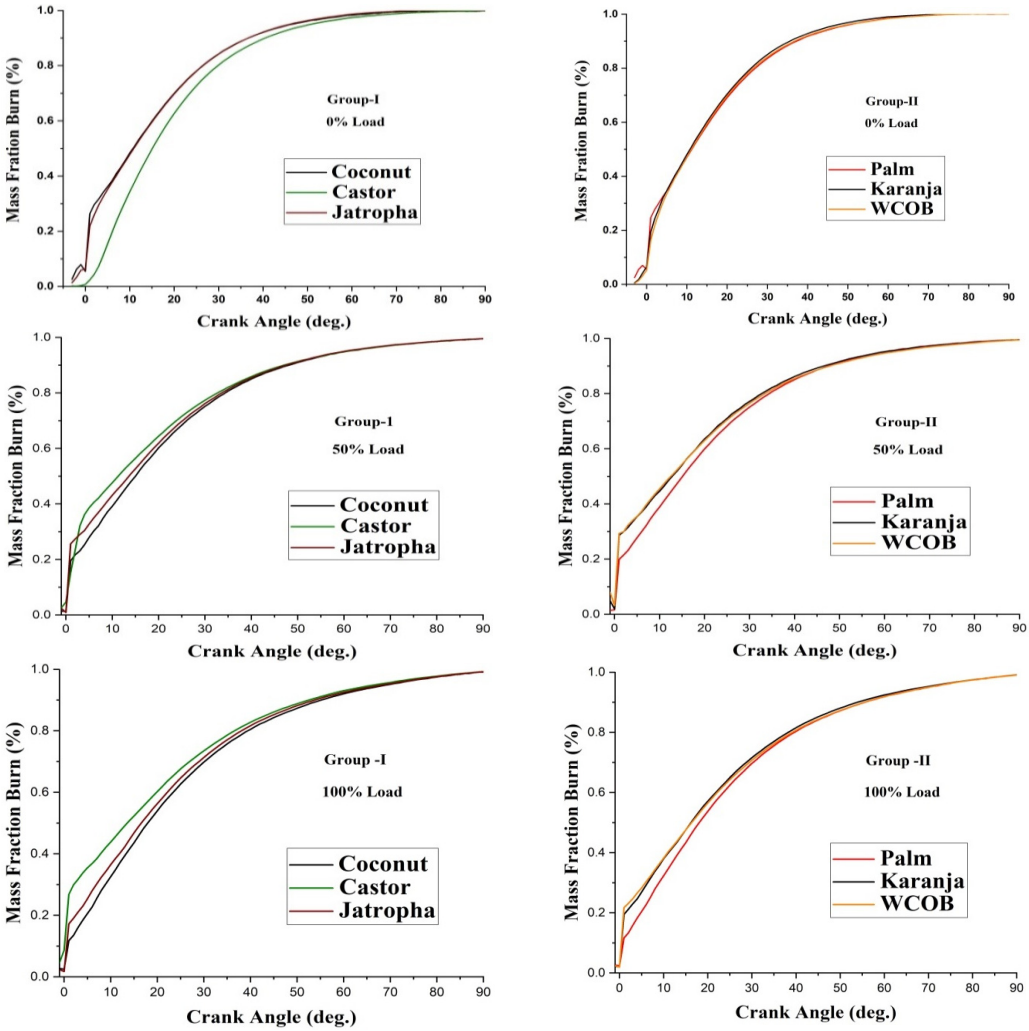

Figure 4. Mass fraction burnt rate for various biodiesels at 0%, 50%, and 100% load.

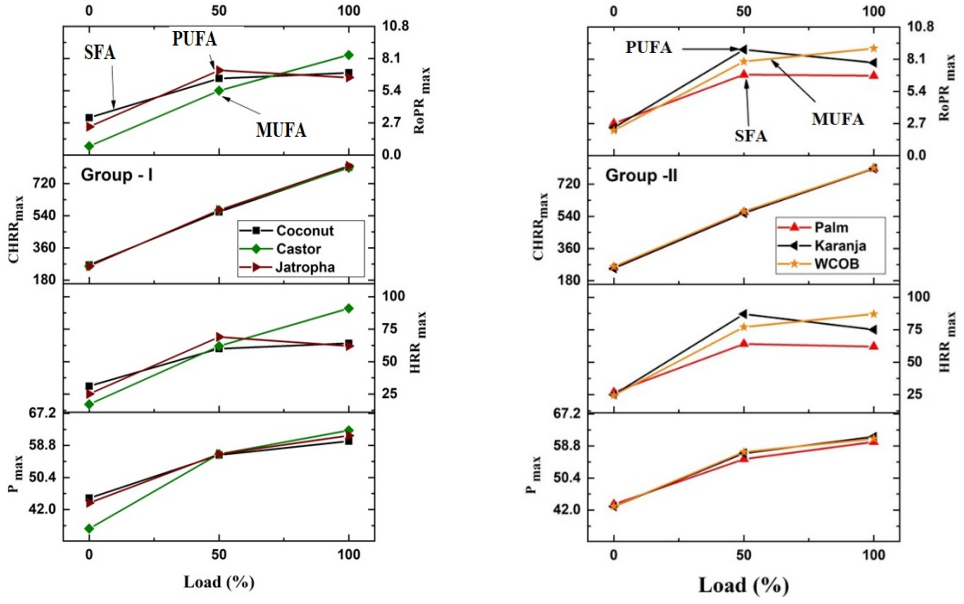

Figure 5. Variation in peak in-cylinder pressure (bar), HRRmax (kJ/m^3), CHHR ((kJ/m^3), and RoPR (bar) at 0%, 50%, and 100% loads.

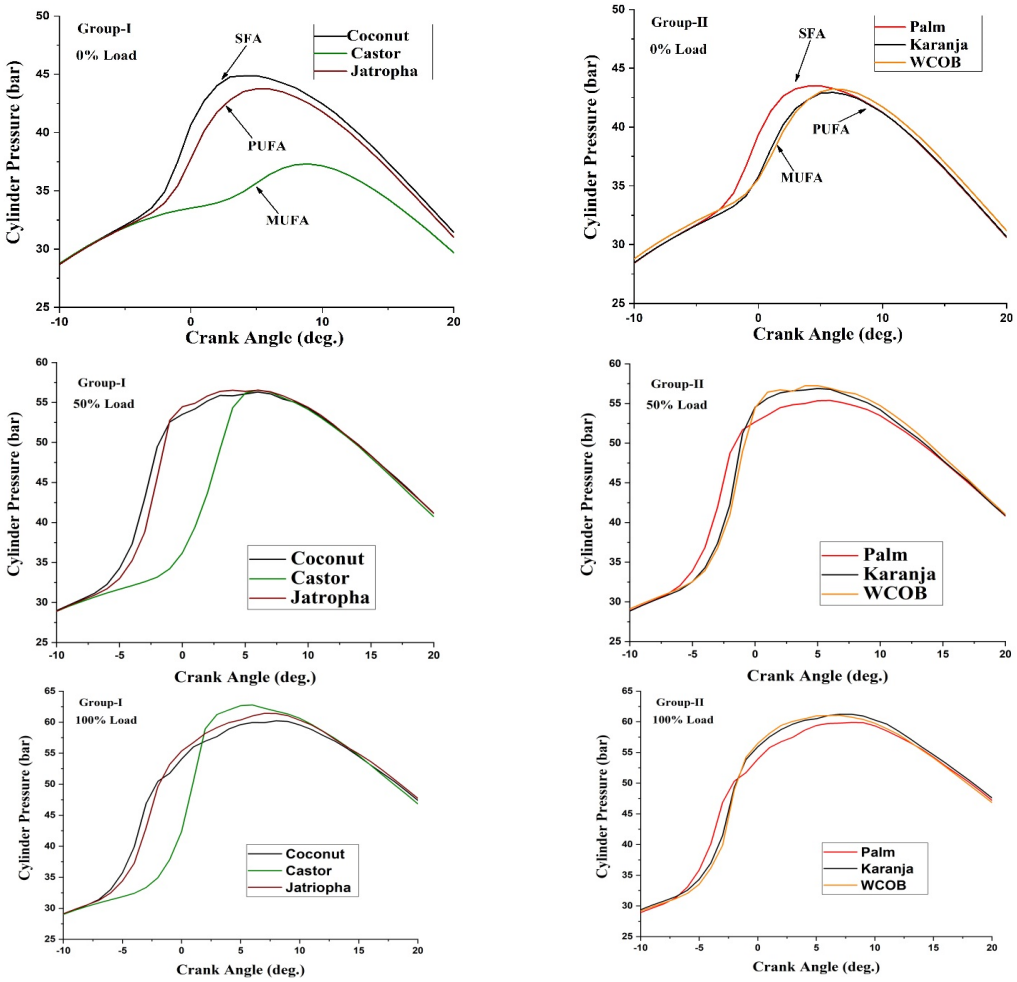

Figure 6. Variation of in-cylinder pressure as a function of engine load and biodiesel type.

3.2.3. The Rate of Pressure Rise

The rate of pressure rise (RoPR) can be used to evaluate the smoothness of the combustion process in the engine cylinder [25]. For lower engine noise and longer engine life, the maximum pressure rate should be as low as possible [25]. The increment in the maximum rate of pressure rise (RoPRmax) was observed as engine load increased (Figure 4). In group I, the RoPRmax was found to be lowest for castor biodiesel at 0% and 50% load condition, but higher at 100% load (Figure 5). When compared with jatropha and castor biodiesel, coconut biodiesel produced 76% and 26% higher RoPR at 0% load, respectively (Figure 7). This characteristic was induced by the higher SFA percent, cetane number, and lower kinematic viscosity of coconut biodiesel as compared with castor and jatropha (Table 4). At 50% load, jatropha gave 9.5% and 23% higher RoPR than coconut and castor biodiesels. However, castor biodiesel produced 17% and 22% higher RoPR as compared with coconut and Jatropha, respectively, at 100% engine load (Figure 7). Jatropha and castor biodiesel both have a higher viscosity and lower CN due to a high USFA% [25]. Higher viscosity affects the fuel spray characteristics such as atomization and evaporation, whereas low CN causes a delay in the SoC. These effects led to an increased ID period (Figure 3) [26]. At full engine load, in-cylinder temperature was higher, which improved the fuel evaporisation and air/fuel mixing rate to make a combustible mixture. Owing to the longer ID, more fuel was accumulated in the premix combustion phase and burned at the same time, which results in higher Pmax and HRRmax (Figure 5) as well as rapid rise in RoPR. Similarly, in group II, at 0% load, palm biodiesel gave a higher RoPR (2.7 bar) followed by karanja (2.35 bar) and WCOB (2.12 bar). Meanwhile, under the full load (100%) condition, WCOB produced a higher RoPR (9 bar) followed by karanja (7.8 bar) and palm (6.7 bar) as shown

in Figure 7. Castor biodiesel and WCOB gave higher RoPR owing to the longer ID period and higher in-cylinder temperature at 100% load (Figure 3).

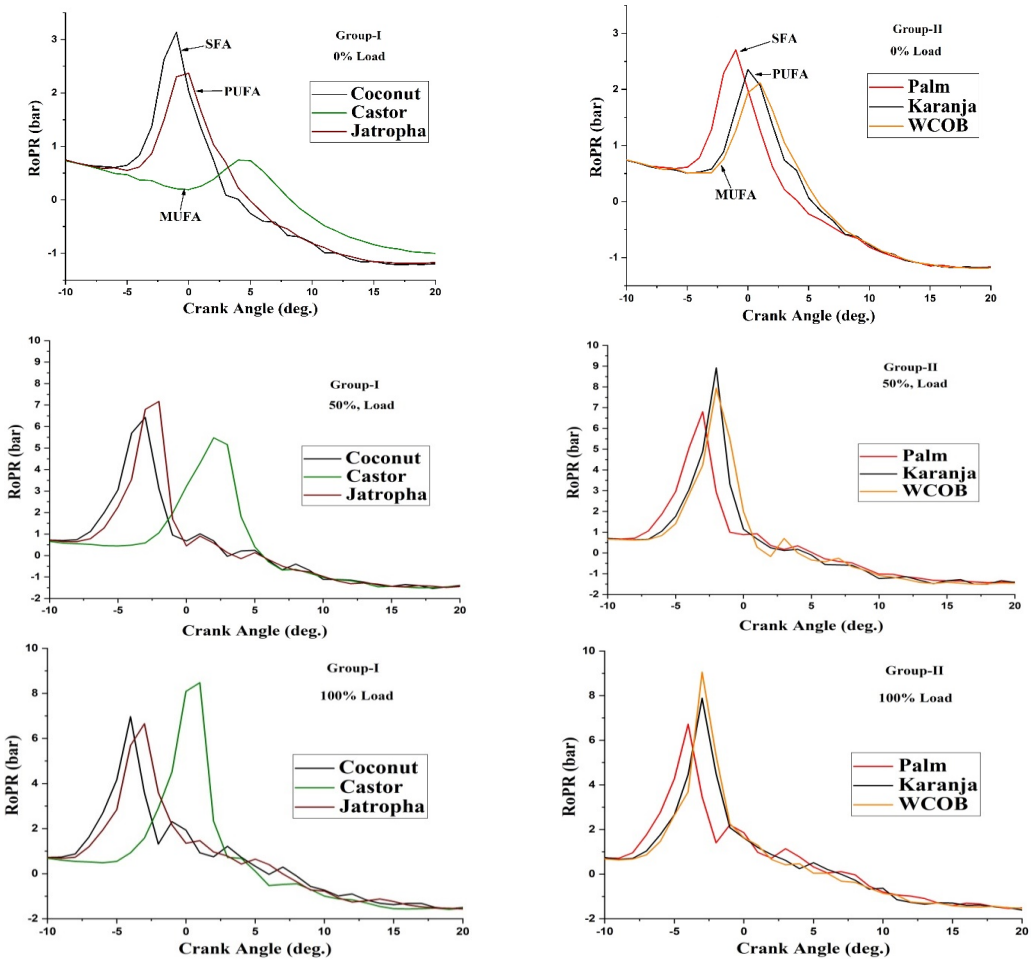

Figure 7. Rate of pressure rise as a function of engine load and biodiesel type.

3.2.4. Heat Release Rate

The HRRmax for PUFA fuels increased as the engine loads rose from 0% to 100% in both groups of biodiesels, according to the results. An increase in the in-cylinder temperature at high load accelerated fuel droplet atomization, vaporization, and A/F mixing rate; hence, produced higher HRRmax [27]. In group I and at 0% load, it was observed that coconut biodiesel produced 44% and 19% higher HRR than jatropha and castor biodiesel, respectively (Figure 8). Lower viscosity and higher CN of coconut biodiesel as compared with jatropha and castor biodiesel caused this (Table 4). At 50% load, jatropha gave 13% and 10% higher HRR as compared with coconut and castor biodiesel. Furthermore, under the full load condition, castor biodiesel gave 29% and 31% higher HRR than coconut and jatropha, respectively. Castor biodiesel produced the highest HRRmax under the full load condition (Figure 8). In group II, palm biodiesel gave 6.5% and 8% higher HRR than karanja and WCOB, respectively, at 0% load (Figure 7). Karanja (MUFA) produced 26% and 11% greater HRR than palm biodiesel and WCOB at 50% load, respectively. At full load, WCOB had a 28% and 13% greater HRR than palm biodiesels and karanja, respectively (Figure 8).

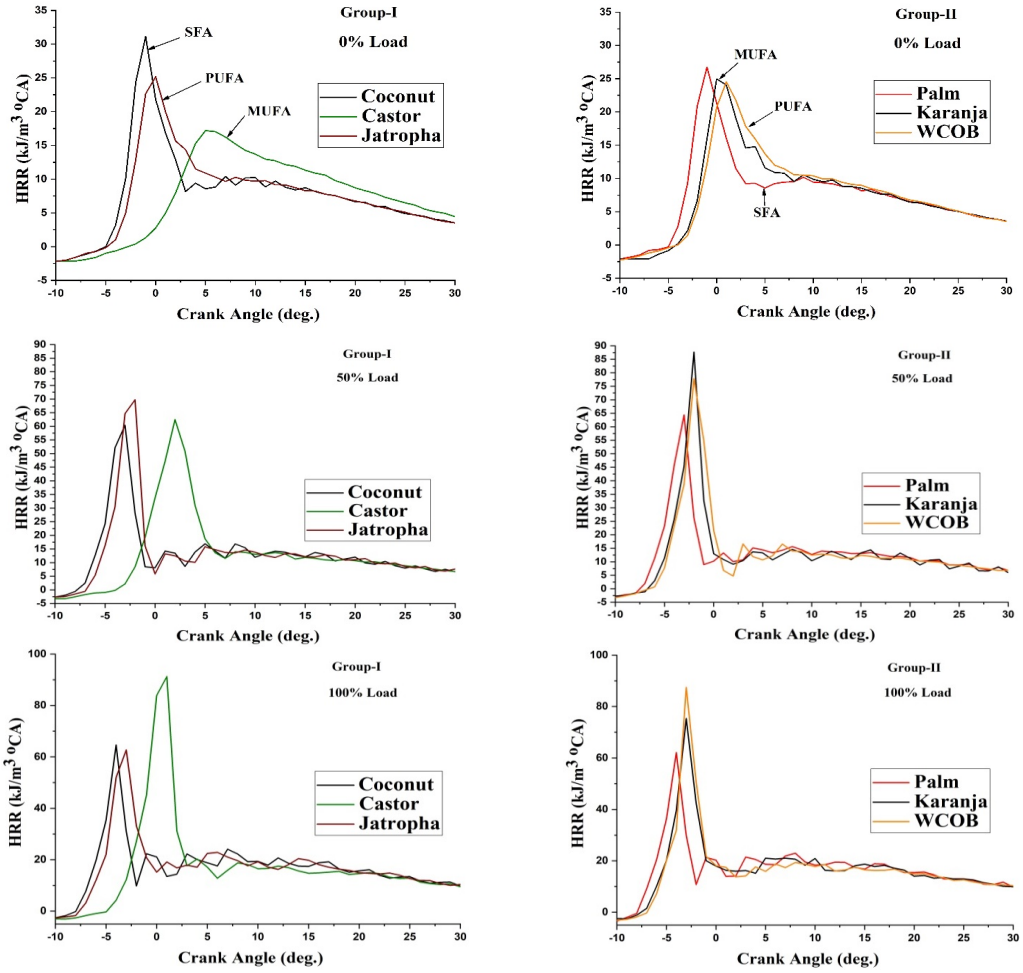

Figure 8. Heat release rate at 0%, 50%, and 100% load.

3.2.5. Cumulative Heat Release Rate

The cumulative heat release rate (CHRR) shows how much heat a fuel creates during combustion. Figure 9 illustrates the CHRR for various biodiesels as a function of engine loads. In group I and at 0% load, coconut biodiesel gave 2.2% and 2.6% higher CHRR as compared with castor and jatropha biodiesel, respectively (Figure 9). No noteworthy changes in CHRR were observed between jatropha (PUFA) and castor (MUFA) biodiesels at high engine load operation. Furthermore, in group II, WCOB showed 1.5% and 3.5% higher CHRR at 0% load, as well as 0.5% and 1.5% at 50% load, than palm and karanja biodiesel, respectively (Figure 9). Meanwhile, at 100% load, no substantial differences were observed in CHRR between the biodiesels in group II (Figure 9). The mass of fuel injected every cycle increased with engine load; hence, the CHRRmax rises (Figure 5), resulting in a faster rate of mass fuel burnt (Figure 4) [28].

3.3. Exhaust Gas Emissions

Many factors influence the types and concentrations of exhaust gases that emerge from an internal combustion engine's tail pipe. Important ones are fuel type and their properties, engine type, as well as other operating parameters such as compression ratio, type of fuel injection (common rail/mechanical), fuel injection pressure, injection timing, injector geometry, combustion chamber volume and geometry, combustion mode, engine load, and engine speed [12,29]. At higher temperatures, nitrogen oxides are formed in the form of NO and NO_2 [12]. N_2 will decompose into highly reactive mono-atomic nitrogen (N) at high temperatures [12]. In group I and at 0% load, it was observed that coconut (SFA) biodiesel gave 88% and 6.6% higher NOx gas emissions than castor (MUFA) and jatropha

(PUFA) biodiesel, respectively (Figure 10). Coconut biodiesel lies in the high SFA group, with a high percentage of shorter carbon chain (C8:0, C10:0, C12:0) (Table 5). These shorter carbon chain fatty acids take less time to break down into smaller molecules and burn at a faster rate as compared with biodiesels containing double bonds (-C=C-) [15]. Hence, higher released energy at low in-cylinder temperature results in higher NOx emissions [15]. However, at 50% load, jatropha (PUFA) biodiesel gave 14% and 18% higher NOx emission than coconut (SFA) and castor (MUFA) biodiesel, respectively. A higher heat release rate at high loads caused higher NOx gas emissions (Figures 8 and 9) [30]. At 100% load, castor (MUFA) gave 15% and 6.5% higher NOx emission than coconut and jatropha, respectively. This occurred because of a combination of increased in-cylinder temperature and a longer ID time (Figure 3). Furthermore, a similar trend was observed in group II; at zero load, palm biodiesel (SFA) gave 11% and 25% higher NOx emissions than those of karanja and WCOB biodiesels, respectively, as shown in Figure 10, whereas at 50% load, karanja (MUFA) produced 13% and 11% higher NOx emissions than palm and WCOB biodiesel, respectively. Furthermore, at full load, WCOB produced 8.3% and 3% higher NOx emissions than palm and karanja biodiesels, respectively.

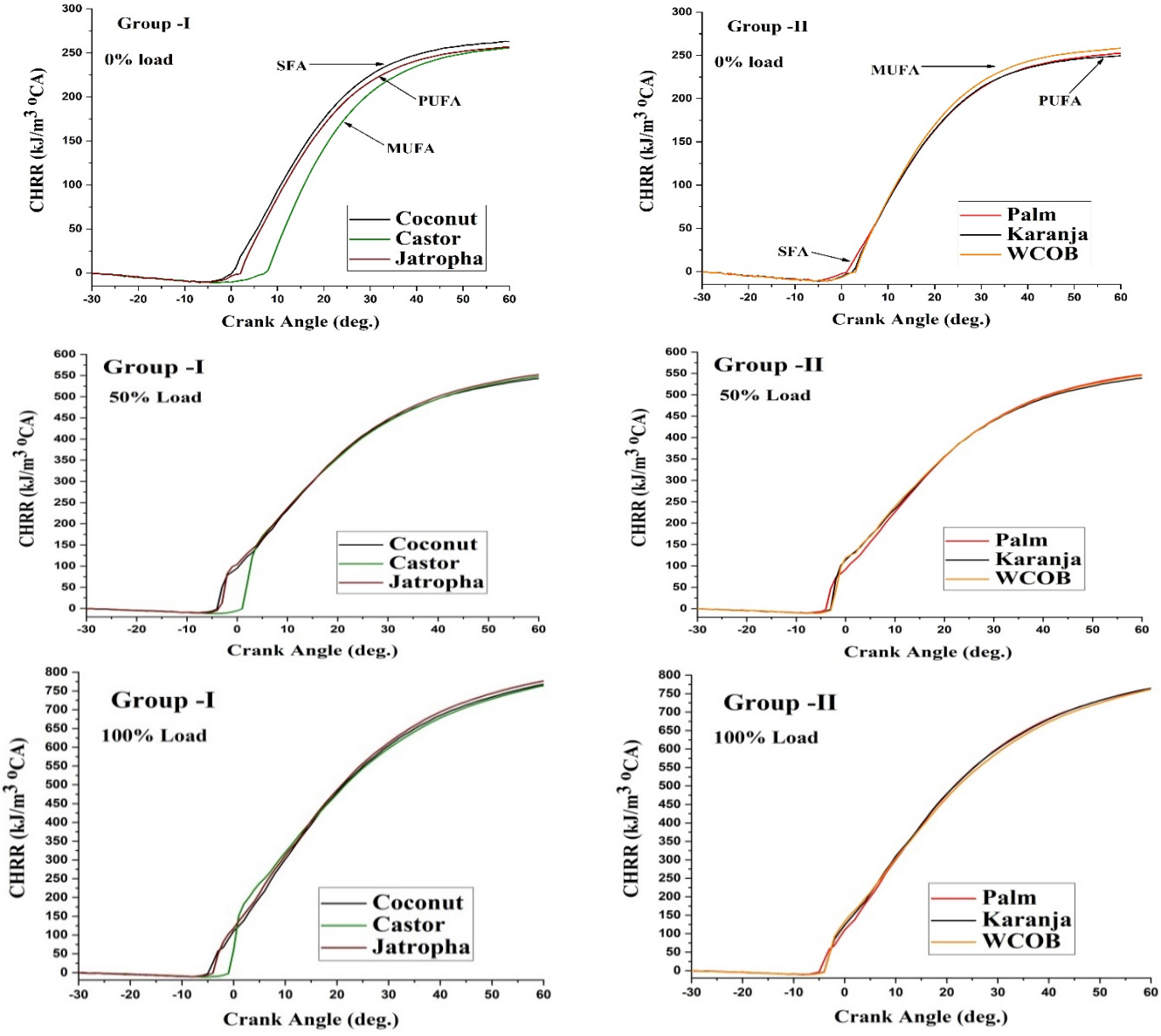

Figure 9. Cumulative heat release at 0%, 50%, and 100% load.

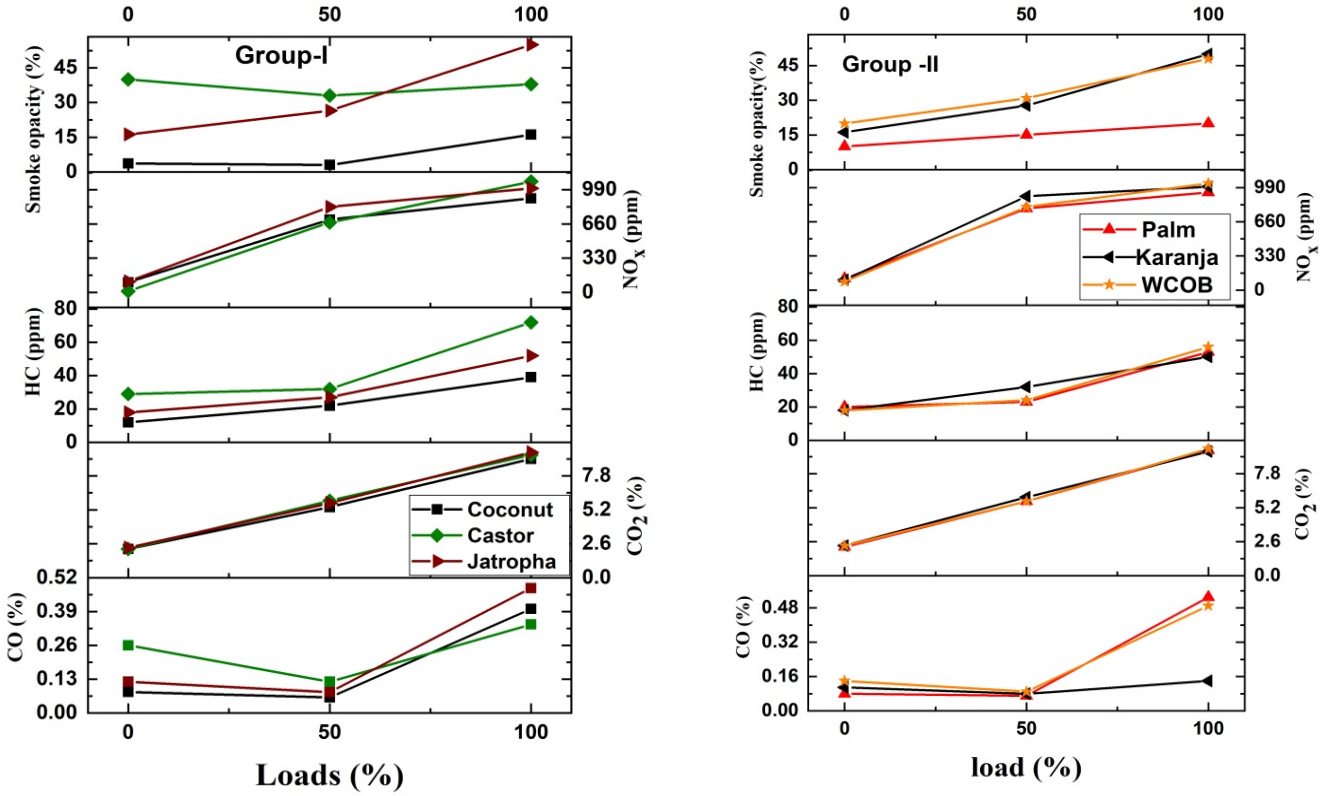

Figure 10. Exhaust gas emissions as a function of engine load and biodiesel type.

In general, NOx gas emissions increased as the degree of unsaturation of biodiesel fuels increased, as did engine loads, as shown in Figure 11. This observation is in line with the literature [31,32]. At 50% load, NOx formation for SFA (coconut, palm), MUFA (karanja), and PUFA (WCOB, jatropha) fuels showed a clear relation with the DU (Figure 11a). However, the NOx emission was found to be relatively lower for castor biodiesel, which falls into the MUFA group (Figure 11a). This unexpected behavior for castor biodiesel was believed to be due to higher viscosity, lower CN, and lower in-cylinder temperature at 50% load. At 100% load, NOx emission increased with DU (Figure 11b). The ID period for PUFA is longer than for SFA and MUFA (Figure 3). Meanwhile, under full load, the high in-cylinder temperature causes more gasoline to vaporize faster and form a combustible combination with air, resulting in more fuel burning in the pre-mixed combustion phase. As a result, NOx emissions from PUFA and MUFA biodiesels increased (Figure 11b). The smoke opacity of coconut biodiesel (SFA) was found to be lower than castor (MUFA) and jatropha (PUFA) biodiesel in group I by 92% and 77% at 0% load; 93% and 88% at 50% engine load; and 52% and 70% at full load, respectively (Figure 10). A high percentage of PUFA caused incomplete combustion and led to higher smoke emissions. A similar result was observed in group II type biodiesels; palm (SFA) biodiesel produced the lowest smoke emission at all engine loads.

An incomplete combustion causes the formation of CO emission, because of the lower oxidation temperature and residence time required for CO_2 conversion [33]. The CO emission for SFA (coconut and palm biodiesel) was found to be lower than for MUFA and PUFA fuels (Figure 10). In group I, coconut biodiesel (SFA) produced lower CO formation by about 79% and 33% at 0% load, as well as 50% and 25% at 50% load, as compared with castor and jatropha biodiesel, respectively. It was believed that a high SFA content and lower viscosity of coconut biodiesel promoted combustion, and hence produced lower CO (Tables 4 and 5) [22,34]. However, at 100% load, coconut biodiesel gave 17% higher CO emissions than castor and 16% lower emissions than jatropha biodiesel. Jatropha biodiesel produced 29% higher CO emissions than castor at 100% load. Meanwhile, in group II, palm

biodiesel (SFA) gave lower a CO emission by about 27% and 42% at 0% load, as well as 30% and 12% at 50% load, than karanja and WCOB, respectively. Whereas at 100% load, palm biodiesel (SFA) produced 73% higher CO than karanja, but 8% lower than WCOB. The CO levels were higher at 100% load owing to increased fuel supply per cycle and a shorter oxidation residence time. CO formation is also influenced by fuel parameters such as density, viscosity, and CN [18,35]. Spray penetration, atomization, and dispersion of high droplet size are all affected by viscosity [26,35]. Because of the larger fuel droplet size and low injection pressure, incomplete combustion occurred, resulting in increased CO emissions [26].

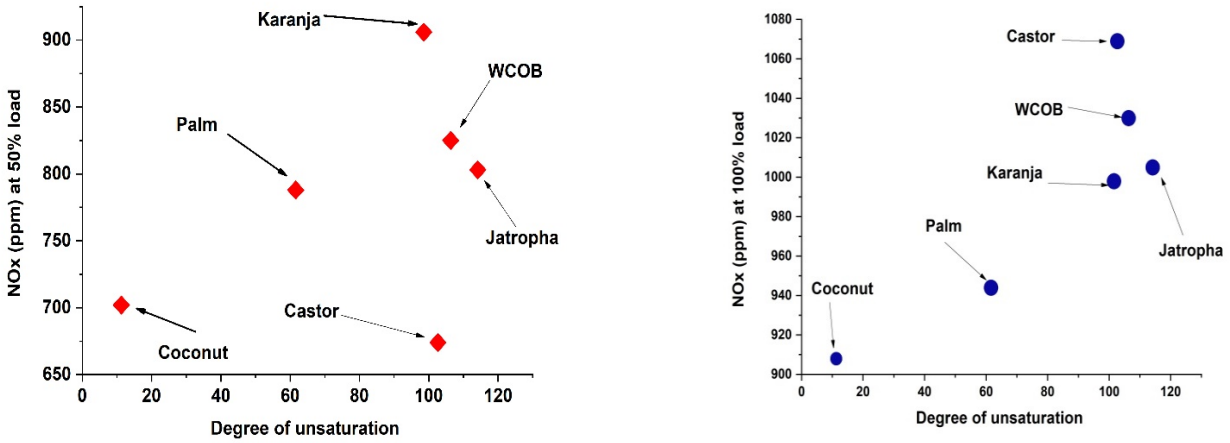

Figure 11. NOx gas emissions with as a function of DU: (**a**) 50% load and (**b**) 100% load.

The increase in engine load increases CO_2 emissions (Figure 10). In group I, CO_2 emissions for coconut biodiesel (SFA) were observed to be lower by 0.02% and 4%, 9% and 5%, and 3% and 5%, at 0%, 50%, and 100% engine load, respectively, as compared with jatropha and castor biodiesel. Meanwhile, in group II, palm biodiesel (SFA) gave lower CO_2 emission by about 4.3% at 0% load, 5% at 50% load, and 1% at 100% load than karanja and WCOB, respectively (Figure 10). Lower viscosity and higher CN of SFA fuels helped to improve the combustion efficiency, which resulted in lower CO_2 emissions (Table 4) [13,35].

The HC emissions of SFA (coconut and palm biodiesel) were found to be lower than MUFA and PUFA fuels (Figure 10). The HC emission was in the sequence of SFA < MUFA < PUFA. Polyunsaturated methyl esters gave a higher HC emission at each engine load condition (Figure 10). At 100% engine load, castor biodiesel (MUFA) gave 45% and 27% higher HC emission than coconut (SFA) and jatropha (PUFA), respectively. The viscosity of castor biodiesel is high, and it contains a higher percentage of ricinoleic acid (C18:1 OH 88%) (Tables 4 and 5). The reactivity of ricinoleic acid is very low as compared with other fatty acids owing to the higher boiling point. Because of these effects, castor biodiesel produced higher HC emissions. In group II and at 100% engine load, HC emissions for WCOB were observed to be 5% and 10% higher than for palm (SFA) and karanja (MUFA) biodiesel, respectively.

4. Conclusions

In this study, various biodiesels were produced and categorized based on their saturation levels (carbon–carbon bonding). Fuel properties were measured and analyzed for highly SFA, MUFA, and PUFA methyl esters. A single-cylinder diesel engine was used to test the combustion and emissions' characteristics. The engine was operated at a constant speed of 1500 rpm and at three different loads (0%, 50%, and 100%). When compared with other fatty acid methyl esters, highly saturated and polyunsaturated fatty acid methyl esters had the best combustion and emission characteristics. The summary of the findings is given below:

(i) As the DU level rises, the viscosity rises as well. Higher viscosity and lower CN are associated with more double bonds in the carbon chain of FAs (–C=C–C–C–C–C–). The viscosity affects the physical delay, while the quantity of double bonds (–C=C–) affects the chemical delay. Because highly saturated biodiesel has a higher cetane number, it ignites more quickly than MUFA and PUFA biodiesels.

(ii) Highly SFA methyl esters show better combustion. At 100% load, coconut biodiesel shows 38% and 3.8% and palm biodiesel shows 10% and 12% advanced SoC as compared with MUFA and PUFA biodiesels, respectively. The ID was found to be about 19% shorter for coconut biodiesel and 5% and 6% shorter for palm biodiesel, as compared with MUFA and PUFA biodiesels, respectively, at 100% load. The SFA gave lower Pmax, 4.7% and 2.4% lower for coconut biodiesel and 2.2% and 1.4% lower for palm biodiesel, when compared with MUFA and PUFA biodiesels, respectively, at 100% load. Coconut and palm produced lower RoPR at 50% and 100% load owing to higher CN and lower viscosity, whereas castor biodiesel and WCOB gave higher RoPR owing to a longer ID period and higher in-cylinder temperature at 100% load.

(iii) PUFAs (jatropha and WCOB) gave better combustion at medium (50%) load as compared with MUFAs (karanja and castor biodiesel). Castor biodiesel showed poor performance at 0% and 50% engine load owing to higher viscosity and low cetane number as compared with other biodiesel samples.

(iv) The NOx, HC, CO, CO_2, and smoke emissions were found to be lower for SFA biodiesels. The coconut biodiesel gave up to 15% and palm biodiesel gave up to 12% lower emissions when compared with MUFA and PUFA biodiesels. The exhaust emission results were found in the order of SFA < PUFA < MUFA. It was observed that jatropha biodiesel gave 70% and 38% high smoke emission than coconut (SFA) and castor (MUFA), respectively, at 100% load.

(v) The unsaturated fatty acids are more reactive than SFA as the double bond increases the reactivity level. Higher UFA methyl ester leads to higher NOx emission. Out of the six biodiesels samples, overall, coconut biodiesel gave the best results under high SFA type biodiesels (group 1). On the other hand, jatropha biodiesel gave better results under the highly unsaturated type of biodiesels (group 2). While selecting biodiesel for diesel engine application, one should try to avoid biodiesel with a high MUFA content.

Engine experiments using different operating conditions such as compression ratios, injection pressures, and exhaust gas recirculation are recommended as a future study. Comparison of the engine performance characteristics is another item of future work. Investigations using other combustion modes such as RCCI and HCCI are other important areas of further research.

Author Contributions: Conceptualization, V.S., A.K.H. and G.D.; methodology, V.S., A.K.H. and G.D.; test rig preparation, V.S. and G.D.; validation, V.S., A.K.H. and G.D.; formal analysis, V.S. and A.K.H.; investigation, V.S., A.K.H. and G.D.; resources, A.K.H. and G.D.; data curation, V.S.; writing—original draft preparation, V.S. and A.K.H.; writing—review and editing, A.K.H. and G.D.; visualization, V.S., A.K.H. and G.D.; supervision, A.K.H. and G.D.; project administration, A.K.H. and G.D.; funding acquisition, A.K.H. and G.D. All authors have read and agreed to the published version of the manuscript.

Funding: The study was funded by the DST-UKIERI project (Grant Number: DST-UKIERI 18-19-04): Waste to Energy-Low Temperature Combustion of Sustainable Green Fuels.

Institutional Review Board Statement: Not applicable.

Informed Consent Statement: Not applicable.

Conflicts of Interest: There are no conflict of interests. The funder was not involved in the study's design, data collection, analysis, or interpretation; manuscript preparation; or the decision to publish the findings.

Nomenclature

bTDC	Before top-dead-center
CN	Cetane number
CD	Combustion duration
$CHRR_{max}$	Maximum cumulative heat release rate
CI	Compression ignition
DU	Degree of unsaturation
EoC	End of combustion
FAME	Fatty acid methyl ester
FAs	Fatty acids
GC-MS	Gas chromatography and mass spectrometer
HC	Hydrocarbon
HRRmax	Maximum heat release rate
ID	Ignition delay
MUFA	Mono-unsaturated methyl ester
MFB	Mass fraction burnt
PUFA	Poly-unsaturated fatty acid
Pmax	Maximum peak pressure
RoPRmax	Maximum rate of pressure rise
SFA	Saturated fatty acids
SoC	Start of combustion
VCR	Variable compression ratio
WCOB	Waste cooking oil biodiesel

References

1. Manojkumar, N.; Muthukumaran, C.; Sharmila, G. A comprehensive review on the application of response surface methodology for optimization of biodiesel production using different oil sources. *J. King Saud Univ. Eng. Sci.* **2020**, in Press. [CrossRef]
2. Hossain, N.; Razali, A.N.; Mahlia, T.M.I.; Chowdhury, T.; Chowdhury, H.; Ong, H.C.; Shamsuddin, A.H.; Silitonga, A.S. Experimental investigation, techno-economic analysis and environmental impact of bioethanol production from banana stem. *Energies* **2019**, *12*, 3947. [CrossRef]
3. Cavalcante, F.T.T.; Neto, F.S.; de Aguiar Falcão, I.R.; da Silva Souza, J.E.; de Moura Junior, L.S.; da Silva Sousa, P.; Rocha, T.G.; de Sousa, I.G.; de Lima Gomes, P.H.; de Souza, M.C.M.; et al. Opportunities for improving biodiesel production via lipase catalysis. *Fuel* **2021**, *288*, 119577. [CrossRef]
4. Naveenkumar, R.; Baskar, G. Process optimization, green chemistry balance and technoeconomic analysis of biodiesel production from castor oil using heterogeneous nanocatalyst. *Bioresour. Technol.* **2021**, *320*, 124347. [CrossRef] [PubMed]
5. Jacob, A.; Ashok, B.; Alagumalai, A.; Chyuan, O.H.; Le, P.T.K. Critical review on third generation micro algae biodiesel production and its feasibility as future bioenergy for IC engine applications. *Energy Convers. Manag.* **2021**, *228*, 113655. [CrossRef]
6. Ewunie, G.A.; Morken, J.; Lekang, O.I.; Yigezu, Z.D. Factors affecting the potential of Jatropha curcas for sustainable biodiesel production: A critical review. *Renew. Sustain. Energy Rev.* **2021**, *137*, 110500. [CrossRef]
7. Senave, M.; Roels, S.; Verbeke, S.; Lambie, E.; Saelens, D. Sensitivity of characterizing the heat loss coefficient through on-board monitoring: A case study analysis. *Energies* **2019**, *12*, 3322. [CrossRef]
8. Syafiuddin, A.; Chong, J.H.; Yuniarto, A.; Hadibarata, T. The current scenario and challenges of biodiesel production in Asian countries: A review. *Bioresour. Technol. Rep.* **2020**, *12*, 100608. [CrossRef]
9. Sakthivel, G.; Nagarajan, G.; Ilangkumaran, M.; Gaikwad, A.B. Comparative analysis of performance, emission and com-bustion parameters of diesel engine fuelled with ethyl ester of fish oil and its diesel blends. *Fuel* **2014**, *132*, 116–124. [CrossRef]
10. Zhu, L.; Cheung, C.S.; Huang, Z. Impact of chemical structure of individual fatty acid esters on combustion and emission characteristics of diesel engine. *Energy* **2016**, *107*, 305–320. [CrossRef]
11. Li, A.; Ji, W.; Huang, Z.; Zhu, L. Predictions of oxidation and autoignition of large methyl ester with small molecule fuels. *Fuel* **2019**, *251*, 162–174. [CrossRef]
12. Puhan, S.; Saravanan, N.; Nagarajan, G.; Vedaraman, N. Effect of biodiesel unsaturated fatty acid on combustion character-istics of a DI compression ignition engine. *Biomass Bioenergy* **2010**, *34*, 1079–1088. [CrossRef]
13. Schönborn, A.; Ladommatos, N.; Williams, J.; Allan, R.; Rogerson, J. The influence of molecular structure of fatty acid mon-oalkyl esters on diesel combustion. *Combust. Flame* **2009**, *156*, 1396–1412. [CrossRef]
14. Kruczyński, S.W. Performance and emission of CI engine fueled with camelina sativa oil. *Energy Convers. Manag.* **2013**, *65*, 1–6. [CrossRef]
15. Zhang, Y.; Yang, Y.; Boehman, A.L. Premixed ignition behavior of C9 fatty acid esters: A motored engine study. *Combust. Flame* **2009**, *156*, 1202–1213. [CrossRef]

16. Selvan, T.; Nagarajan, G. Combustion and Emission Characteristics of a Diesel Engine Fuelled with Biodiesel Having Varying Saturated Fatty Acid Composition. *Int. J. Green Energy* **2013**, *10*, 952–965. [CrossRef]
17. Sharma, V.; Duraisamy, G. Production and characterization of bio-mix fuel produced from a ternary and quaternary mixture of raw oil feedstock. *J. Clean. Prod.* **2019**, *221*, 271–285. [CrossRef]
18. Alviso, D.; Artana, G.; Duriez, T. Prediction of biodiesel physico-chemical properties from its fatty acid composition using genetic programming. *Fuel* **2020**, *264*, 116844. [CrossRef]
19. Dhar, A.; Kevin, R.; Agarwal, A.K. Production of biodiesel from high-FFA neem oil and its performance, emission and combustion characterization in a single cylinder DICI engine. *Fuel Process. Technol.* **2012**, *97*, 118–129. [CrossRef]
20. Sharma, V.; Duraisamy, G.; Cho, H.M.; Arumugam, K.; Alosius, M.A. Production, combustion and emission impact of bio-mix methyl ester fuel on a stationary light duty diesel engine. *J. Clean. Prod.* **2019**, *233*, 147–159. [CrossRef]
21. Jiaqiang, E.; Liu, T.; Yang, W.M.; Li, J.; Gong, J.; Deng, Y. Effects of fatty acid methyl esters proportion on combustion and emission characteristics of a biodiesel fueled diesel engine. *Energy Convers. Manag.* **2016**, *117*, 410–419. [CrossRef]
22. Ruhul, M.A.; Abedin, M.J.; Rahman, S.M.A.; Masjuki, B.H.H.; Alabdulkarem, A.; Kalam, M.A.; Shancita, I. Impact of fatty acid composition and physicochemical properties of Jatropha and Alexandrian laurel biodiesel blends: An analysis of performance and emission characteristics. *J. Clean. Prod.* **2016**, *133*, 1181–1189. [CrossRef]
23. Agarwal, A.K.; Dhar, A. Experimental investigations of performance, emission and combustion characteristics of Karanja oil blends fuelled DICI engine. *Renew. Energy* **2013**, *52*, 283–291. [CrossRef]
24. Rajesh, K.; Natarajan, M.P.; Devan, P.K.; Ponnuvel, S. Coconut fatty acid distillate as novel feedstock for biodiesel production and its characterization as a fuel for diesel engine. *Renew. Energy* **2021**, *164*, 1424–1435. [CrossRef]
25. Hossain, A.K.; Refahtalab, P.; Omran, A.; Smith, D.I.; Davies, P.A. An experimental study on performance and emission characteristics of an IDI diesel engine operating with neat oil-diesel blend emulsion. *Renew. Energy* **2020**, *146*, 1041–1050. [CrossRef]
26. Thomas, J.J.; Manojkumar, C.V.; Sabu, V.R.; Nagarajan, G. Development and validation of a reduced chemical kinetic model for used vegetable oil biodiesel/1-Hexanol blend for engine application. *Fuel* **2020**, *273*, 117780. [CrossRef]
27. Yi, P.; Long, W.; Feng, L.; Chen, L.; Cui, J.; Gong, W. Investigation of evaporation and auto-ignition of isolated lubricating oil droplets in natural gas engine in-cylinder conditions. *Fuel* **2019**, *235*, 1172–1183. [CrossRef]
28. Can, Ö. Combustion characteristics, performance and exhaust emissions of a diesel engine fueled with a waste cooking oil biodiesel mixture. *Energy Convers. Manag.* **2014**, *87*, 676–686. [CrossRef]
29. Hellier, P.; Jamil, F.; Zaglis-Tyraskis, E.; Al-Muhtaseb, A.H.; Al-Haj, L.; Ladommatos, N. Combustion and emissions characteristics of date pit methyl ester in a single cylinder direct injection diesel engine. *Fuel* **2019**, *243*, 162–171. [CrossRef]
30. Garner, S.; Brezinsky, K. Biologically derived diesel fuel and NO formation: An experimental and chemical kinetic study, Part 1. *Combust. Flame* **2011**, *158*, 2289–2301. [CrossRef]
31. Navaneeth, P.V.; Suraj, C.K.; Mehta, P.S.; Anand, K. Predicting the effect of biodiesel composition on the performance and emission of a compression ignition engine using a phenomenological model. *Fuel* **2021**, *293*, 120453. [CrossRef]
32. San José, J.; Sanz-Tejedor, M.A.; Arroyo, Y.; Stoychev, P. Analysis of vegetable oil mixture combustion in a conventional 50 KW thermal energy installation. *Renew. Energy* **2021**, *164*, 1133–1142. [CrossRef]
33. Dhar, A.; Agarwal, A.K. Experimental investigations of the effect of pilot injection on performance, emissions and combustion characteristics of Karanja biodiesel fuelled CRDI engine. *Energy Convers. Manag.* **2015**, *93*, 357–366. [CrossRef]
34. Hosamani, B.R.; Katti, V.V. Experimental analysis of combustion characteristics of CI DI VCR engine using mixture of two biodiesel blend with diesel. *Eng. Sci. Technol. Int. J.* **2018**, *21*, 769–777. [CrossRef]
35. Thomas, J.J.; Sabu, V.R.; Basrin, G.; Nagarajan, G. Hexanol: A renewable low reactivity fuel for RCCI combustion. *Fuel* **2021**, *286*,119294. [CrossRef]